Available online at www.jrors.ir

JRORS
Journal Of Radar and Optic Remote Sensing

Journal Of Radar and Optic Remote Sensing

JRORS 1 (2018) 15–35

Investigation of Urban Biophysical Compounds in the Formation of Thermal Islands Using RS and GIS (Case Study: Yazd)

Sedigheh Emami[a1] , Esmail Emami[b]

[a]*Ms in GIS, remote sensing,Yazd Branch, Islamic Azad University, Yazd, Iran*
[b]*Graduate student University of electric power systems of the Islamic trends free khomeynishahr*

Received 2 December 2017; revised 1 June 2018; accepted 3 June 2018

Abstract

The urban thermal island phenomenon has intensified in recent years due to the changes in urban airspace along with the rise of urbanization. Spatial-temporal patterns of biophysical constituents, which include vegetation, impermeable surfaces and soil type in the city, have a significant impact on urban thermal islands. The purpose of this study is to investigate the role of effective urban parameters in the formation and clustering of Yazd urban thermal islands. In order to achieve the proposed goal, the thermal map was developed using the single-window algorithm on the thermal band of OLT sensor of Landsat ETM+ sensors for August, 2015 and 2017; Land surface temperature (LST) was calculated and using spatial correlation (LISA), hot and cold clusters of thermal islands of Yazd were extracted. In order to evaluate the surface temperature, with the intensity of LST, spatial heterogeneity of the clusters increases nonlinearly. The relationship between the thermal islands with NDVI and urban carrion layers were investigated. Cold clusters are around the places with more green space and hot clusters are in the arid areas and in areas without vegetation cover. The result of the correlation between the surface temperature and the NDVI, NDBI, and NDBaI indicated that the relationship between NDVI and LST is negative, and the relationship between NDBaI and LST is also nonlinear and negative. But the relationship between NDBI and LST is nonlinear and positive. A spatial correlation

* Corresponding author. Tel: +98-9166225978.
E-mail address: s.emami061@gmail.com.

with the local index has emphasized the extent of thermal islands in the studied periods.

Keywords: Urban thermal islands; Ahwaz city; Local spatial correlation index (LISA)

1. Introduction

Urban thermal islands are the phenomenon in which the temperature of urban areas, in comparison with the surrounding rural areas, is evident. This urban phenomenon has intensified due to the change in airspace and with increasing urbanization (Vogt & Oke, 2003; Song & Wu, 2016). Accordingly, humanized activities in urban areas lead to the release of enormous amounts of energy, and this is a major contributor to the climate change of the regions associated with the transformation of energy exchange (Yuna & Bauer, 2007). The importance of urban thermal islands made the researchers and thinkers of the environmental and urban sciences have different definitions and categories of this phenomenon. In one of the divisions, which Voogt and Oke (2003) have of the most important and cited partings of this urban phenomenon, urban thermal islands have three categories:

1. Coating Layer of Thermal Islands. (CLHI) 2. Frontal Layer of Thermal Isles. (BLHI) and 3. Level of Urban Thermal Island. (SUHI). From the first two groups, Teuton was named '*Air Separation Thermal*', which is most often assessed using air temperature records collected from weather stations. While SUHI is recovered more often through surface temperature (LST) and is viewed from remote sensing satellites, it is usually observed with high precision and universal spatial coverage and low cost compared to data collected through water ponds and weather forecasting are very popular .On the other hand, this technology is able to more clearly demonstrate the spatial and metamorphic patterns of urban thermal islands, which reveals the role of biophysical parameters in the formation and management of urban thermal islands (Li et al., 2011; Weng, 2012). As it was said, today remote sensing is an effective tool for understanding urban environments, because with its unique capabilities (i.e. repeating images taken from a region), maps with multiple spatial spaces are made available to the public and the curtains Has found many problems at the micro level (i.e. urban level) (Yuan & Bauer, 2007). Remote Sensing Services does not end there. In particular, the US Geological Survey (USGS) developed the National Land Use Land Cover with the help of TM ETM + imaging sensors, which contributed greatly to thematic interpretation Coverage of land and land use. Since the traditional land cover classification methods failed to meet the growing need for urban studies, analyzes were developed at sub-pixel levels (Deng & Wu, 2012). This method is known from urban studies in the literature of (Vegetation-Impervious surface-soil) or vegetation - impermeable

- soil. Under this conceptual framework, types of land cover (except water) in urban environments can be considered as a combination.

The city's biophysical concept consists of three basic parts: vegetation, impenetrable surface and soil. Accordingly, two groups of different methods have been developed to determine the quantity of urban biophysical compounds: the first group includes methods for learning machine learning: such as the neural network (Mohapatra & Wu, 2008; Pu et al., 2008) Regression and decision tree (Lu & Weng, 2009; Mohapatra & Wu, 2010) and regression models (Yang & Liu, 2005; Yang, 2006). In this method, information derived from spatial and spatial features extracted from remote sensing methods is illustrated with an experimental relationship. The second group consists of separating spectral techniques (Small, 2005; Powell et al., 2008; Weng, 2012). The basic assumption of the present method is that each cell is a combination of several homogeneous sample spectra; the spatial fragmentation coverage of each of the components of the earth can be attributed to the spectral mixture analysis. Previous studies on the relationship between the behavior and prospects of urban thermal islands indicate that the composition and configuration of land cover and its uses in this regard are important from studies (Connors et al., 2013).

Global studies in this area show that the processing of remote sensing data at urban levels has been increasing dramatically in recent years. Cao et al., (2010) evaluated the intensity of the Urban Cooling Island in urban urban parks in Japan using ASTER, IKONOS data. The results of the athletic research in 92 parks in Nagoya showed that the cooling effect is dependent on the size and seasonal seasonal conditions of the park, and the park's size is non-linear to the cooling of its surroundings. Buyantuyev & Wu (2010) investigated the relationship between temporal variations of ground-level temperature with land cover and social and economic patterns in the Sonoran Desert in northern Aryrana. They studied two pairs of images of the day and night in the middle of the year (June) and the semi-cold of the year (October). Their research results showed a significant difference in temperature, due to the high role of vegetation loss. Also finally, using geographic weighted regression, social and economic spatial relationships were assessed with surface temperature, which indicated the positive role of human factors in the formation of thermal islands. The study of the effect of urban biophysical constituents on surface temperatures in the city of Wisconsin, including Washington, Ozaki, Milwaukee and Wakkushah, is a study by Deng and Woo (2013). In this study, they studied the level of the urban thermal islands (SUHI) in the areas mentioned, and concluded that moisture in the soil (wet and dry) had important implications for the SUHI modeling. Although the Deng and Wu’s study presented valuable results in modeling the surface of the island's thermal island (SUHI), it failed to address urban biophysical compositions in modeling clusters of urban thermal islands.

A research that can address the deficiencies and explore a new method while designing research strengths is conducted by Guo et al. (2015) in Guangzhou, Guangdong Province, China. In this study, Numerical Analysis of NDVI, NDBI, NDBaI indices, using spatial correlation index (LISA), extracted clusters of urban thermal islets. They concluded that

the NDVI and NDBI indices had the highest impact on urban thermal island clusters. A survey of the biophysical impact on the urban thermal island was conducted by Song & We (2016) in Wisconsin, USA. The overall result of this study is the unimaginable role of impermeable surfaces in the thermal island diversity of urban areas. Among the studies carried out in Iran, Ahmadi et al. (2012) have been investigating the temporal-temporal variations of thermal patterns in Shiraz. Their results, based on TM image processing and ETM +, showed that the temperature rings of Shiraz conform to the polluted and high-traffic areas of the city and the coldest areas are also consistent with vegetation. Spatial analysis of Shiraz's temperature during the warm and cold season with an emphasis on statistical and satellite processing is also a research that Ahmadi et al. (2015) have focused on. The output of this study showed that in the warm season, the lowest temperature thresholds were consistent with vegetation, but in the cold season, the northern and northwest regions, which dominated the new settlements and the northwest highlands, which dominated the new settlements and altitudes The northern part of the city has been matched. Considering that documentary research has not been conducted with the approach of urban biophysical combinations and the spatial correlation index, the present research has focused on this issue. To this end, we have proposed strategies to prevent the spread of thermal islands in Yazd.

2. Materials and Methods

2.1. Area of study

Yazd is located at 31" and 55 ◌́ north, 54 " and 20 ◌́ east. The height of Yazd is 1218 meters above sea level. Yazd is located in the dry and semi-dry belt of the Northern Hemisphere. Yazd city is located in a wide, dry and enclosed valley between Shirkouh and Kharanag mountains. (Fig 1)

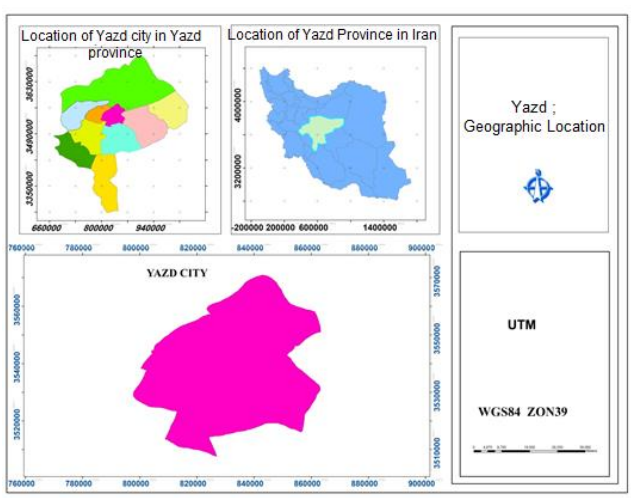

Fig 1. Area of study

2.2. Materials

This research is an analytical method. But it should be added in terms of purpose. In the applied dimension, the results can be used in decision making and planning. To extract the surface temperature of the city of Yazd, the data from the thermal images of the ETM + Landsat satellite is used. One of the most important analytical steps in this study is to convert the digital value of the image to spectral radiance (Chander and Groeneveld, 2009). The steps for estimating the surface temperature are as follows, which are explained below: 1. Convert the digital value of the image to the spectral radiance; 2. Convert the spectral radiance to the brightness temperature. 3. Conversion of light temperature to kinetic temperature (Chander & Markhan, 2003). In the third step, the correction of the earth surface temperature emission for the conversion of light temperature to kinetic temperature was calculated according to the equations of Li et al. (۲۰۱۱) and Sobrino et al. (2004). To assess the vegetation situation, some indicators have been proposed, the most common and most accurate of which are the NDVI index (Atzberger, 2013), and the capabilities of this indicator were used in this study. Also, in order to evaluate other urban biophysical parameters, the Normalized Difference Build-up Index (NDBI) and Normalized Difference Bareness Index (NDBaI) were worked out.

In this study, the land surface temperature evaluation process using Landsat 8 satellite images was presented in MATLAB software in three stages including preprocessing of image, calculating ground temperature and estimating frequency of plant using spectral composition linear analysis.

Step 1 (Preprocessing the image): This study should be performed on triangles 4, 5 and 10 on non-cloudy days. At this stage, geometric and atmospheric corrections are usually done to accurately calculate the surface temperature of the earth.

Step 2 (calculating ground temperature): The researchers were able to find a meaningful relationship between these factors by examining different light spectra and reflecting them at different temperatures and reflection of phenomena. In this regard, it is possible to use the Landsat 10, which is a thermal infrared image.

In fact, this reflects the thermal reflection of phenomena as a black body. In order to find the surface temperature, the temperature of the satellite or the temperature of the black body must first be obtained and then, with the two methods mentioned above, the surface temperature of the earth can be calculated. Calculation of satellite effective temperature: At this stage, digital numbers are first converted into spectral sensors using Equation (1).

$$L_\lambda = \frac{(Lmax - Lmin) \times DN}{2 \times 5} + \text{offset} \quad (1)$$

The Lmax, Lmin and offset values are extracted using metadata. Then, the satellite effective temperature at this stage will be obtained from equation (2):

$$T_S = \frac{T_S}{in(^{K_1}/_{L_\lambda} + 1)} \quad (2)$$

In this equation, TS is the effective temperature of the satellite or the illumination temperature of the sensor. K1 and K2 are correction coefficients that have values of 666.09 and 1287.71 respectively (for Landsat images). The temperature of this stage is also known as black body temperature.

Calculation of ground surface temperature: Two methods can be used to calculate ground surface temperature.

The single-window algorithm was developed to provide surface temperature image of the earth. Although atmospheric correction still needed. This algorithm requires three parameters: the emissivity, transmission and atmosphericity. The average atmospheric temperature of the single-window algorithm is calculated using equation (3) (Yang & Liu, 2005).

$$T = \frac{1}{C[a(1 - C - D) + (b(1 - C - D) + C + D)T_S - DT_a]} \quad (3)$$

In this equation, Ts is the effective temperature of the satellite and Ta is the average atmospheric temperature that can be obtained by a simple equation with near-surface temperature (Ta). The coefficients a and b have a value of -67/355351 and 0/458606, respectively. Also, C and D are derived in equations 4 and 5.

$$C = t\varepsilon \quad (4)$$

$$D = (1- t) [1+ (1-\varepsilon) t] \quad (5)$$

In these equations, t is an atmospheric transition that can be estimated using near-surface temperature and water vapor data as well as meteorological observations of the area. Based on the findings, there is always a linear relationship between t and water vapor (Zhang et al, 2007).

The t-value and the average atmospheric temperature can be estimated according to Qin studies (Qin et al., 2003 and 2001). In fact, each of the land leakage has a certain specific flux determined by their Snyder study (Snyder, 1998). With the detection of a minimum

NDVI for coated areas and a maximum NDVI for areas with a dry soil, a range for NDVI was obtained in other areas. If we accept that the plants have a greater reflection in the infrared band than the red band, then NDVI for plants will always be positive. Therefore, identification of the outer soil cells can be made in NDVI smaller than or equal to zero (SalmanMahini and Kamyab, 2009). Therefore, with the average of soil irradiance and vegetation cover, we can calculate the dissipation of other areas from Equation (6):

$$\varepsilon = \varepsilon_v PV + \varepsilon s\,(1- \varepsilon_v) + d\varepsilon \quad (6)$$

In this equation, Emissivity are areas with a full coverage and areas with a dry soil. Also, calculating the effect of surface distribution is possible using Equation (7).

$$D\varepsilon = (1-\varepsilon_s)\,(1-F)\,\varepsilon v \quad (7)$$

F is a form factor in this equation whose mean value based on different geometric distribution is 0.55. Also, the percentage of vegetation cover can be obtained from Eq. (8).

$$PV = \left[\frac{NDVI - NDVI_{min}}{NDVI_{max} - NDVI_{min}}\right]^2 \quad (8)$$

Corrected ground temperature: In this method, the ground surface temperature is obtained from Equation (9) in terms of Kelvin (Artis & Carnahan, 1982)

$$T = \frac{T_S}{1 + \left(\lambda \times \frac{T_S}{(P)In\varepsilon}\right)} \quad (9)$$

In this regard, the wavelength of the radiation radiated is 11.5 μm.

Also, (1.438 × 10-2 Km) p = hc / σ, j / K is Boltzmann's constant, h is the Planck constant, and equal to 6.626 × 10-34 and c is the light speed with 2.998 × 108 m / s.

2.3. Preparing indicators maps

Stage 3 (calculating ground temperature and estimating frequency of plant using spectral composition linear analysis (P8) (P LSMA)): Rid (1995) used the V-I-S model to parametrizate the urban biophysical composition.

This model was later used in many studies due to its valuable results from the description of urban composition and dynamics (Yang & Liu, 2005).

The V-I-S model is used with NDVI, NDIs and NDBAIs for urban land classification (Weng et al, 2004). By providing these three images, we can better understand a combination of city users.

There are significant variations in the spectra of each floor covering. After normalizing, the amount of light shifts can be eliminated or reduced, although much information will be reduced. The normal reflection of each bond is obtained by using equation (11) (Yang & Liu, 2005).

The NDBI[1] index is calculated using the following equation. This indicator indicates the built areas.

$$\text{NDBI} = \frac{SWIRI - NIR}{SWIRI + NIR} \quad (10)$$

Preparing NDBaI[2] Map for Yazd City:

Using the following equation, the NDBaI is calculated. This indicator indicates the arid areas.

$$\text{NDBaI} = \frac{SWIRI - TIRSI}{SWIRI + TIRSI} \quad (11)$$

In the above relationships, SWIR represents the infrared wavelength band and the TIRS is thermal band.

Preparing NDVI Map for Yazd City:

This index was calculated in the field emission calculations. NDVI represents the vegetation cover.

After calculating the ground surface temperature with single-window and NDVI-Emissivity algorithms and NDBI indices, NDBaI, using MATLAB software, selects 3,017 dots randomly in images obtained from NDBI, NDBaI, NDVI indices, and surface temperature. Extract image information in selected points with Exteract by value to point, in ArcGIS software. Then, we analyze the correlation between NDBI, NDBaI, NDVI and LST indices in SPSS software. To analyze the spatial statistics, the temperature of the surface of the earth and the thermal islands has been used from the local Moran index.

3. Results

Statistical analysis of surface temperature in Yazd city

By reviewing the data on the surface temperature of Yazd in August, the two study periods (2015 and 2017) showed that the surface temperature is decreasing (Table 1), so that the minimum temperature from 25.717601 Celsius in 2015 decreased to 18.98599 Celsius in 2017. The average temperature has dropped by 5.3 degrees Celsius, with a maximum temperature of 55.4741 degrees Celsius in 2015 to 51.2445 degrees Celsius in

---

[1] - Normalized Difference Build-up Index (NDBI)

[2] - Normalized Difference Bareness Index (NDBaI)

2017. The maximum temperature of the studied courses has also decreased significantly. The difference between the years (2015-2017) was 4.23 degrees Celsius. In the studied period, mode in 2015 has changed dramatically, but in 2017 there is no significant difference with two statistics.

Table 1. Statistical indexes of the surface temperature of Yazd

2017	**2015**	**Statistics**
3017	3017	N
41.41731805	46.711420857	Mean
.078651793	.0811714129	Std. Error of Mean
42.48099900	47.745998000	Median
43.254902	51.8032990	Mode
4.320124725	4.4585204236	Std. Deviation
18.663	19.878	Variance
-1.226	-1.156	Skewness
.045	.045	Std. Error of Skewness
1.886	1.585	Kurtosis
.089	.089	Std. Error of Kurtosis
29.900401	28.2581000	Range
18.98599	25.717601	Minimum
51.2445	55.4741	Maximum
124956.048549	140928.3567250	Sum

Spatial relationships modeling

This tool models the relationships between variables that are related to geographic complications and allows us to predict the values of unknown variables and better understand the factors that affect a variable. Regression methods allow us to examine the relationships between variables and measure the severity and weakness of those relationships.

Space relationship analysis tool

Geographic weighted regression: Geographical weight regression is a local model of the variable or process that one is trying to understand. Geographic weighted regressions do this by providing separate regression equations for each complication by considering dependent and independent variables that are complicated throughout the band (i.e. range).

Geographic weighted regression is a technique used for descriptive analysis of spatial statistics. The equation is written as follows (Rezaei, 2017)

$$YI=\beta 0+\beta 1X1+\varepsilon \quad (12)$$

In this equation, y is a dependent variable, β is the coefficient of correlation, X is independent variable and ε is random error.

Correlation coefficients

One of the basic definitions in the science of statistics is the definition of correlation and the relationship between the two variables. In general, we define the correlation as the severity of the dependence of the two variables on each other. There are many types of different correlation coefficients, each measuring the correlation between the two variables according to the type of data and the conditions of the variables. In general, the correlation coefficients vary between -1 and +1, and the relationship between the two variables can be positive or negative. Correlation coefficient is a reciprocal relationship, the more correlation coefficient is closer, the greater the degree of dependence of the two variables.

Pearson correlation coefficient

This correlation coefficient is based on covariance of two variables and their standard deviations, which can be used to calculate the Pearson correlation coefficient.

$$r_{xy}=\frac{cov(x,y)}{\sigma_x\sigma_y} \quad (13)$$

Table 2. Pearson correlation coefficient between land surface temperature (LST) and NDBAI, NDVI, NDBI

Pearson Correlation	LST	NDVI	NDBAI	NDBI
LST	1	-.230**	-.525**	.232**
NDVI	-.230**	1	.111**	-.235**
NDBAI	-.525**	.111**	1	.020
NDBI	.232**	-.235**	.020	1

**. Correlation is significant at the 0.01 level (2-tailed).

In this study, the relationships between NDVI and LST were negative, since the distribution of these two parameters in the city did not have a uniform dispersion. A strong and negative relationship occurs between two parameters when the city or its surface has one-handed cover or it has a gradual decrease. The results of the evaluation of the temperature are a good confirmation that the relationship between NDVI and LST, or

between NDBI and LST, is not necessarily linear or non-linear. The relationship between NDBaI and LST is also negative. However, NDBI and LST have a positive relationship. (Fig2)

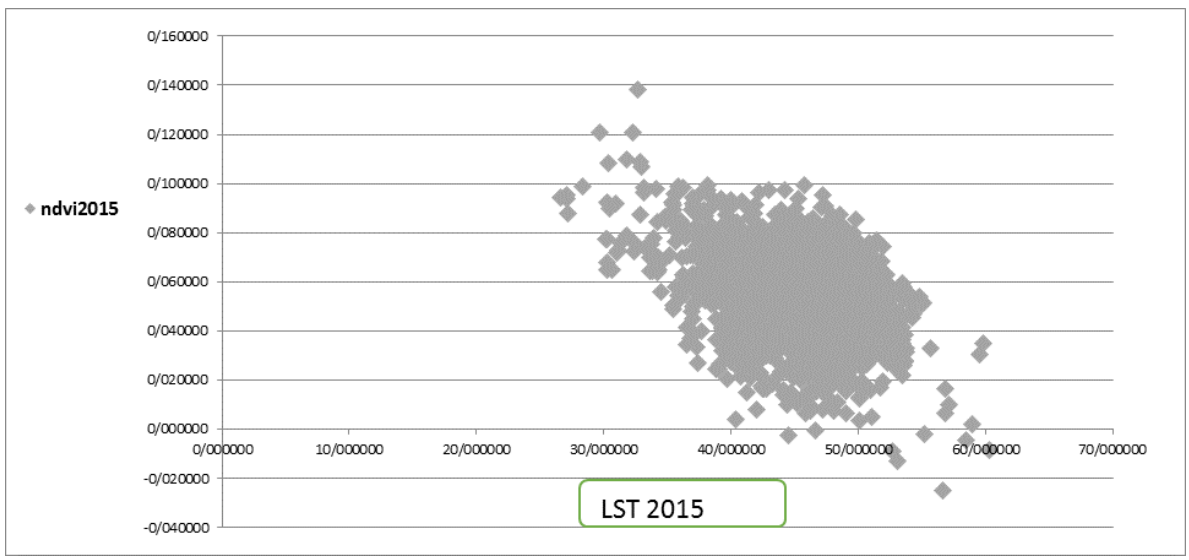

Fig2.A. The relationship between LST and NDVI in 2015

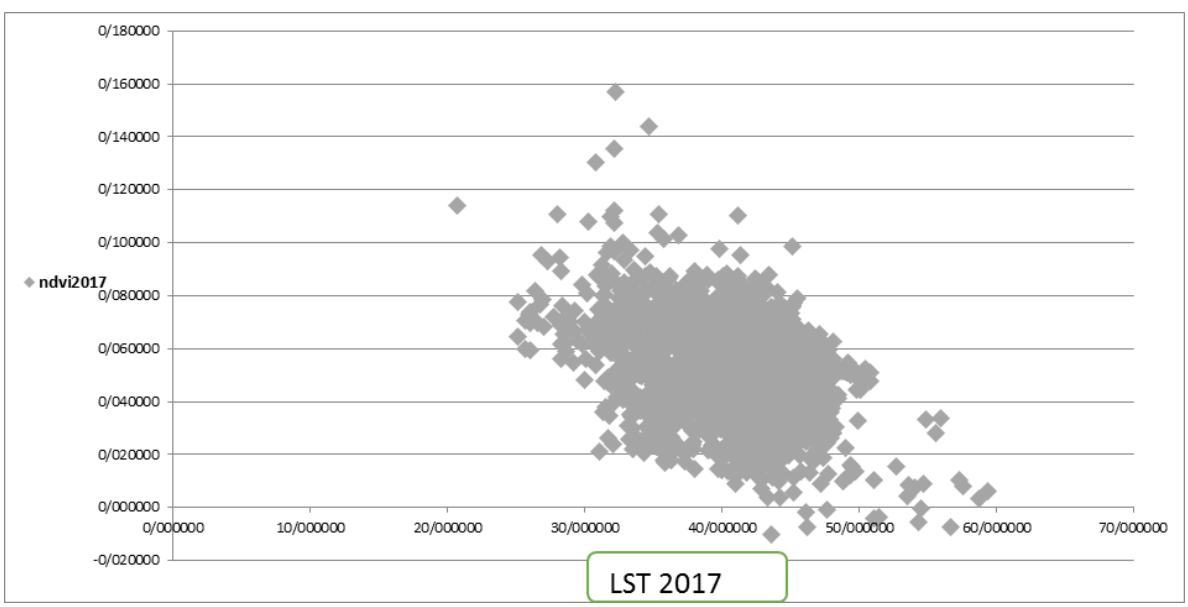

Fig2. B. The relationship between LST and NDVI in 2017

The temperature range for August 2015 and 2017 on (Fig. 3) shows a fundamental change in ground temperature for a minimum and a maximum. The lowest temperature in 2015 is 25.71 degrees Celsius and in 2017 it is 18.98 degrees Celsius. The maximum temperature in 2015 is 55.47 degrees Celsius and in 2017 it is 51.24 degrees Celsius. The minimum temperature is shown with cream color and the maximum temperature with blue.

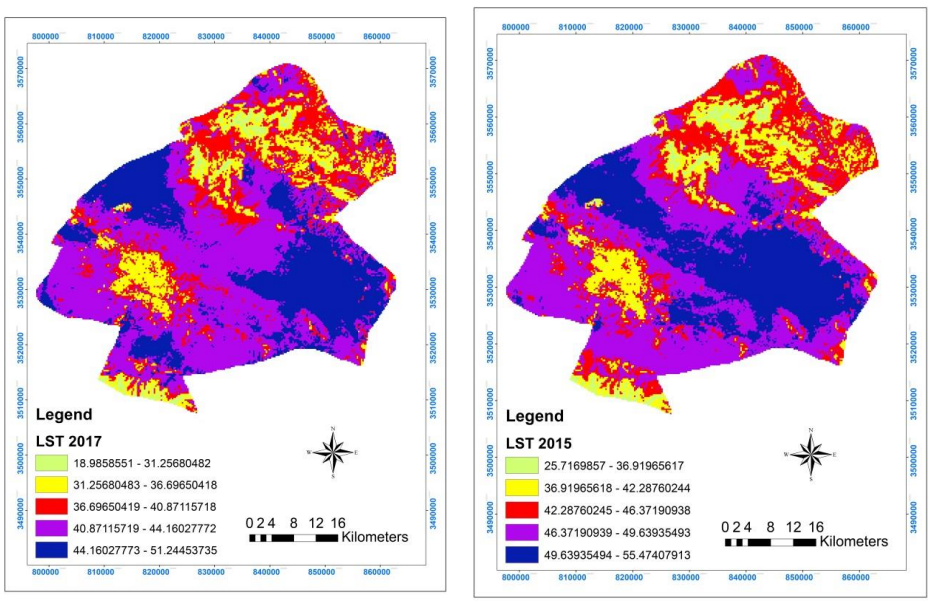

Fig3. Land surface temperature (2017 and 2015

The comparison of the temperature with the vegetation shows that the hot spots are in the arid areas and the areas without vegetation. They are marked with red dots, while the cold spots are marked with green dots (Fig. 4).

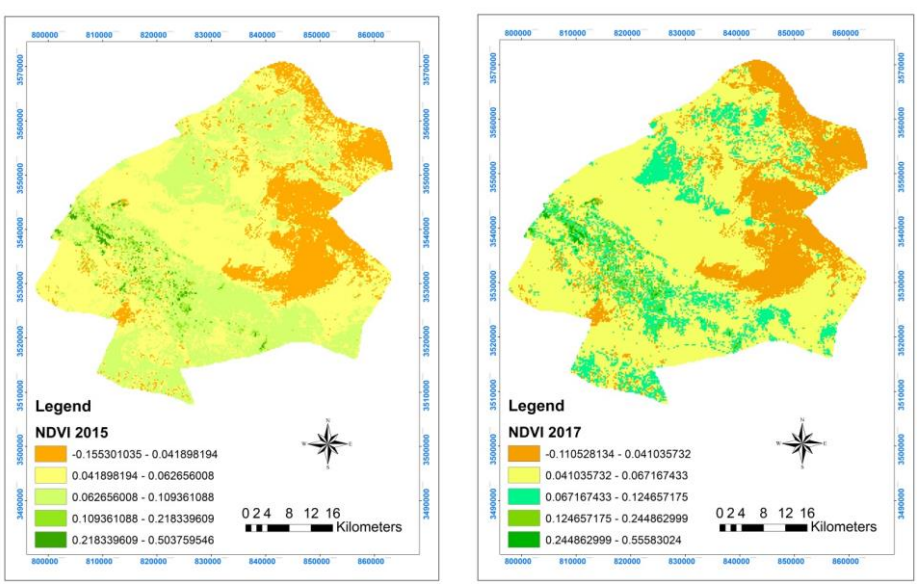

Fig4. Vegetation (2015 and 2017)

Spatial statistics in the ArcGIS environment

This analysis is based on spatial data and its basic function is to obtain information that is necessary so that planners move towards statistical-graphing of locational data. Perhaps the misconception about GIS is that it is a kind of software. It is not true because GIS is considered as a powerful system for planning and specialized software is used for it (Rezaei, 2017).

To carry out the spatial analysis, four important and practical parts for implementing spatial variations that include relevant steps are given.

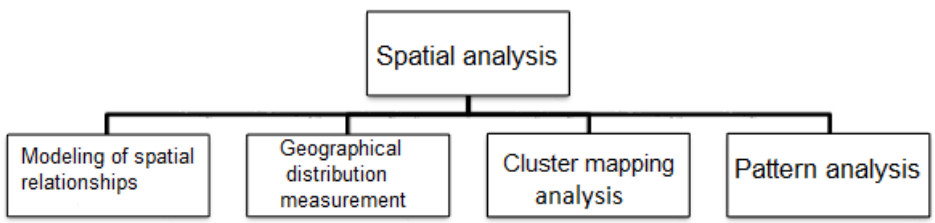

Pattern analysis

To investigate the spatial pattern of data, we can use the Moran index to determine the quantity and test the spatial structure. The Moran index examines autocorrelation based on the location of the two values and analyzes the geographical condition in that location (Griffith, 1987). In order to calculate the Moran index, the z and p-value scores are firstly calculated, and in the next step, the evaluation and significance of the index are examined (Fisher and Gates, 2009). ArcGIS 10.3 software has been used to calculate spatial autocorrelation using the Global Moran index. If the Moran index is close to +1, the data are spatial autocorrelation and cluster pattern and if the Moran index is close to -1, the data are dispersed.

Cluster mapping analysis

If we have a set of weighting effects, this tool identifies clusters of points with similar and different values of size. Creating a map of clusters, especially when it comes to the location of one or more clusters, is very useful. Unlike methods and tools that show trends and general patterns and produce figures and statistics, cluster mapping tools allow us to visualize clusters (Rezaei, 2017).

Analysis of hot and cold clusters

If we have a set of weighting effects, this tool identifies the clusters of complications with high amounts (or hot clusters) and clusters of complications with low amounts (or cold clusters).

Analysis of hot and cold clusters of urban thermal islands has been performed from the local Moran index. This index classifies the temperature values of the earth's surface in the form of a warm / cold cluster in places close to each other and most closely resembling it (Anslin et al., 2006). Therefore, this study was carried out to determine the clusters of urban thermal islands after obtaining the temperature of the surface of the earth.

The cluster revealed by this method has shown the relationship between urban thermal islands and urban biophysical compounds on a city scale. The local Moran is calculated from the following equation.

$$I_i = n \times \frac{(x_i - \bar{x})}{\sum_i (x_i - \bar{x})^2} \times \sum_j w_{ij}(x_i - \bar{x}) = \frac{z_i}{m_o} \times \sum_j w_{ij} z_j, \quad \text{with:} \quad m_0 = \sum_i \frac{z_i}{n},$$

(14)

In the above equation, X_i is the property of i, X is the average of the desired property and W_{ij} is the spatial weight between the i and j components. The points generated by this statistic, along with the significance of local Moran, produce four categories of distribution of dispersion, which a user and scientific scholar can use to determine their spatial correlation type of their data. These four categories of information are as follows:

Hot thermal islands (HH): This type of thermal islands represents areas where the surface temperature of earth (LST) is much higher than the average surface area of the entire area.

Cold thermal islands (LL): This type of thermal islands represents areas where the surface temperature of earth is lower than the average of the entire area.

Hot thermal islands near cold thermal islands (HL): This type of thermal islands represents areas where the surface temperature of earth is high, while the temperature of adjacent regions is lower than the average of the entire area.

Cold thermal islands near warm thermal islands (LH): This type of thermal islands represents areas where the surface temperature of earth is low, while the temperature of adjacent regions is higher than the average of the entire area.

In addition to the four types of thermal islands, the output of this function may have a fifth type, which is briefly depicted as NS (meaningless). Areas with such a degree actually show that there was no significant local connection at the surface temperature of that area.

This tool also detects spatial clusters. To do this, this tool calculates the local Moran value, Z score, P value and a code that indicates the type of cluster for each complication. The Z score and P value represent a significant amount of calculated index (Rezaei, 2017).

Geographic distribution measurements

. Spatial autocorrelation of surface temperature in Yazd city (Global Moran Index)

Autocorrelation relates to the relationship of residual values along the regression line. Autocorrelation is based on the first law of geography and randomness (random). This tool, in fact, specifies the Moran index. The Moran statistic is expressed using a correlation coefficient, and its orbit varies between +1 and -1. Hence, if its value moves to +1, it shows a high and concentrated cluster pattern in most of the studied areas. If it moves to -1, it will represent a dispersed pattern on the geographic side. If Moran is close to zero, it means that autocorrelation does not exist, and this indicates a random and non-significant pattern at the desired level of confidence (Ahmadi, Dadashiroudbari, 2016).

-1<Moran<+1

In order to evaluate spatial autocorrelation, the surface temperature data of Ahwaz with a spatial scale of 30 meters were used. Table 3 shows the global Moran autocorrelation values for the Earth's surface temperature. As it is illustrated, surface temperature in Yazd has a positive spatial autocorrelation in all studied years. We conclude that the surface temperature data of Yazd have a space structure and are distributed in the form of a cluster. According to Table 4, the temperature distribution pattern of Yazd is in a hot-hot cluster pattern.

Table 3. The output of Moran statistics for Yazd city

Global Moran's I Summary	2017	2016	2015
Moran's Index:	0.79	0.85	0.83
Expected Index:	-0.0003	-0.0003	-0.00
Variance	0.0002	0.0002	0.0002
z-score	51.53	55.20	53.57
p-value	0.00	0.000	0.00

Table 4. Temporal distribution pattern of the region

Distribution pattern type	**p-value**	**z-score**	**Number**
Strong cluster - cold – cold	0.01	-2.58>	1
Medium cluster - cold – cold	0.05	(1.96-)-2.58-	2
Weak cluster - cold – cold	0.1	(1.65-) - 1.96-	3

Random - Distorted Distribution	.....	1.65 - 1.65 -	4
Weak cluster - hot – hot	1.65	1.96-	5
Medium cluster - hot – hot	0.05	2.58-1.96	6
Strong Cluster - Hot – Hot	0.01	2.58<	7

. Local Indicator of Spatial Coherence

As discussed earlier, the Global Moran Space Autocorrelation function specifies only the type of surface temperature pattern. For this reason, to show the spatial distribution of the governing pattern of the thermal islands of Yazd and its clustering during the studied period, the local correlation is used. In this statistic, HH represents clusters of high surface temperature values (positive spatial correlation at 99% confidence level), LL denotes clusters of low surface temperature values (negative spatial correlation at 99% confidence level). On this basis, as shown in Table 6, the cluster of thermal warming is 12,600 meters in 2015 and 14,670 meters in 2017, and finally 27,270 meters in area of Yazd city. The cold thermal islands also have 14850 meters in 2015 and 15720 meters in 2017 from the city's atmosphere. Areas lacking an autocorrelation pattern are also presented in Table 6. These regions depict urban biophysics in the formation of thermal islands because of the high changes in the surface temperature in the findings and its high contrast in the city of Yazd. In fact, this function only reveals the thermal islands that are most likely to focus and cluster in space.

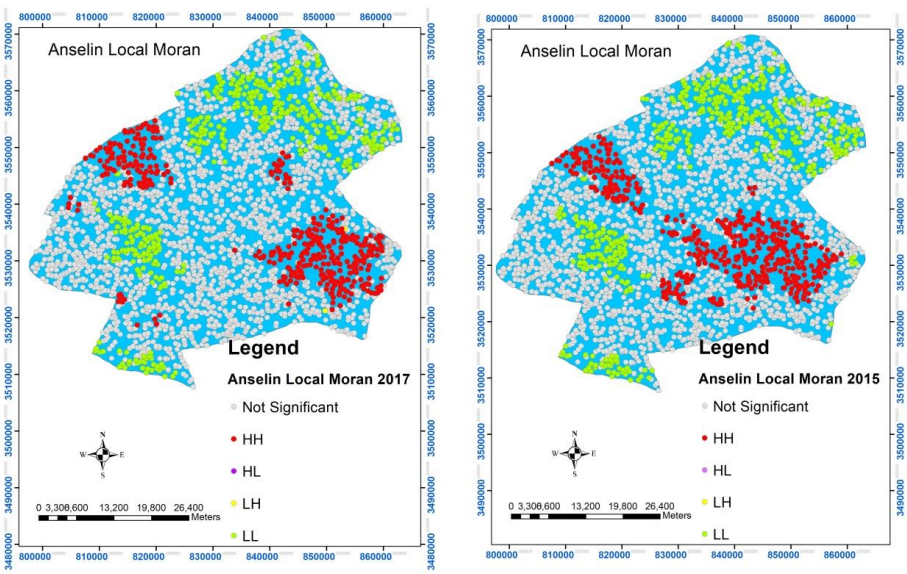

Fig 6. The Moran index of Yazd in 2015 and 2017

Table 6. Area under thermal island cluster coverage (m)

Pattern type	2015	2017
Hot thermal islands (HH)	12600	14850
Cold thermal islands (LL)	14670	15720
No significant pattern (NS)	63150	59910

. Spatial Relations Modeling

Multiple regression

The correlation coefficient (R2) in 2015 between the variables is 0.595, which indicates that there is a relatively high correlation between the variables. Also, the adjusted R Square value of 0.593 indicates that 59 percent of the total temperature variation in Yazd is dependent on these three variables used in this equation.

The regression equation of 2015:

(15) Lst2015 = 46.86-19.76 * NDVI- 13.98 * NDbai + 25.09 * NDbi

The correlation coefficient (R2) in 2017 between variables is 0.582, which shows that there is a relatively good correlation between the variables. Further, the Adjusted R Square value of 0.574 indicates that 57 percent of the total temperature variation in Yazd is dependent on these three variables used in this equation.

The regression equation of 2017:

(16) Lst2017 = 41.66 -18.71 * NDVI- 13.56 * NDbai + 22.09 * NDbi

4. Conclusion and Discussion

Earth surface temperature plays a crucial role in the exchange and interaction of energy flux between the surface and the air; therefore, understanding the link between LST and the features of the urban surface is critical to designing effective measures to reduce the thermal island range.

This study was carried out with an innovative and object-oriented approach using spatial correlation index with the aim of investigating the effects of urban biophysical parameters on the formation and clustering of urban thermal islets of Yazd. For this purpose, OLS sensor images of Landsat 8 were received in August 2015 and 2017 from the US Earth Science Foundation (USGS), and the surface temperature of each of the images was calculated for the Yazd area. In the next step, three indicators of NDVI, NDBI, and NDBai were calculated and their results were studied to evaluate the biophysical combinations of Yazd.

The results indicate that the two NDVI and NDBi indices have a significant correlation with LST so that the NDVI index has a negative effect on LST whereas, conversely, NDBi has a positive effect. It was found that two NDBai and NDVI indices are good indicators for studying urban thermal islands.

In this study, it was found that the distribution of NDVI and LST clearly revealed both warm and cold edges in Yazd, in such a way that the relations between these two parameters in the city do not have a uniform dispersion. The strong negative relationship between these two parameters occurs when the city or surface of it has a uniform coverage or gradual decrease, which is another claim for the structural interaction of city thermal islands.

The results of the spatial autocorrelation of the global Moran show that the temperature data of the Yazd has a structured pattern and is distributed in the form of strong hot-hot clusters. That is, high temperatures and low temperatures tend to be concentrated or clustered in space.

The results of clustering the urban thermal islands with local Moran function showed that in the course of time, the size of warm thermal islands has increased and consequently the size of the cold islands has also increased. The changes in the earth surface temperature of Yazd have contributed to the disappearance the order of clustering of the thermal islands, but the extent of areas with such a statistical characteristic (lacking statistical significance) has reduced. As noted, based on the type of urban management features, the results of this research in the area clearly help urban planners to reduce the effects of Yazd urban thermal islands.

A comparison of the results of this study with the research carried out by Wang (2012) and Yang and Baer (2007) showed that Heat has a positive relationship with the city's biophysical properties, and the temperature has a positive relationship with impenetrable surfaces and a negative relationship with the coating There is a green plant that has a logical relation to the results of this research. Lee et al. (2011) showed that the development of urbanization has an impact. ISA and NDVI have a positive effect on urban thermal islands, and the relationship between the distributions of LST coverage pattern indicates the direct relation of LST to Land, which is consistent with the results of this research. The study by Xiao and Modi (2005) showed that the temperature in urban areas was directly related by distributing the land cover pattern, which is consistent with the findings of this research. Comparison of the results of this study with Ahmadi et al. (2012 and 2015) and Gao et al. (2015) have shown that due to the simultaneous application of multivariate partitioning methods in order to reduce the complexity of urban space and spatial correlation function, this research has better explained the clusters of thermal islands.

References

Ahmadi, M. And Ashoorl, d., Mandans Fred, M., 2015, Analysis of the temperature of Shiraz city in hot and cold seasons using statistical analyzes and satellite images.Geographic Quarterly Journal, Year 30, Issue 2, pp. 147-160.

Ahmadi, M. And Ashoorl, d., Mandans Fred, M., 2012, Temporal and temporal variations of thermal and user patterns in Shiraz city using TM & ETM sensor data, Remote Sensing and GIS, 2009, 4 (4), pp. 55-68.

Ahmadi, M. and Dasashi roudbari, A., 2016. Effects of Biophysical Compounds on the Formation of Urban Thermal island (Case Study: Mashhad), Remote Sensing and GIS,No. 8, autumn 2015, pp. 39-58.

Anselin, L, Syabri, I and Kho,Y, 2006. GeoDa: An Introduction to Spatial Data Analysis, Geographical Analysis, Geographical Analysis, 38(1), pp.2-22.

Artis, D. A. & Carnahan, W. H. 1982. Survey of emissivity variability in thermography of urban areas. Remote Sensing of Environment, 12: 313–329.

Atzberger, C., 2013, Advances in Remote sensing of Agriculture: Context Description, Existing Operational Monitoring Systems and Major Information Needs, Remote Sensing, 5(2), pp.949-981.

Buyantuyev, A. & Wu, J., 2010, Urban Heat Islands and Landscape Heterogeneity: Linking Spatiotemporal Variation in Surface Temperatures to Land-cover and Socioeconomic Patterns, Landscape Ecology, 25(1), pp. 17-33.

Cao, X., Onishi, A., Chen, J. & Imura, H., 2010, Quantifying the Coll Island Intensity of Urban Parks Using ASTER and IKONOS Data, Landscape and Urban Planning, 96(4), pp. 224-231.

Chander, G. & Groeneveld, D.P.,2009, Intraannual NDVI Validation of the Landsat 5 TM Radiometric Calibration, International Journal of, Remote Sensing, 30(6), pp. 1621-1628.

Chander, G. & Markham, B., 2003, Revised Landsat-5 TM Radiometric Calibration Procedures and Postcalibration Dynamic Ranges, LEEE Transition on Geoscience and Remote Sensing, 41(11), pp. 2674-2677.

Connors, J.P., Galletti, C.S.& Chow, W.T., 2013, Landscape Configuration and Urban Heat Island Effects: Assessing the Relationship between Landscarpe Characteristics and Land Surface Temperature in Phoenix, Arizona, Landscarpe Ecology,28(2), 271-283.

Deng, C. &Wu, C., 2012, BCI: A Biophysical Composition Index for Remote Sensing of Urban Environment, Remote Sensing of Environment, 127. pp.247-259.

Deng, C & Wu, C., 2013, Examining the Impacts of Urban Heat Island: A Spectral Unmixing and Thermal Mixing Approach, Remote Sensing of Environment, 131. pp.262-274.

Fischer, M.M.& Getis, A. ,2009, Handbook of Applied Spatial Analysis: Software Tools, Methods and Applications, springer Science & Business Media.

Griffith, D. A. (1987). Spatial Autocorrelation: A Primer (Washington, DC: Association of American Geographers). Resource Publications in Geography.

Guo, Wu, Z., Xiao, R., Chen, Y., Liu, X., & Zhang, X., 2015, Impacts of Urban Biophysical Composition on Land Surface Temperature in Urban Heat Island Clusters, Landscape and Urban Planning, 135, pp.1-10.

Li, J., Song,C.,Cao,L.,Zhu,F.,Meng,X. & Wu,J.,2011,Impacts of Landscape structudy of Shangai, China, Remote Sensing of Environment , 115(12), pp.3249-3263.

Liu L, Zhang Y. 2011. Urban Heat Island Analysis Using the Landsat TM Data and ASTER Data: A Case Study in Hong Kong. Remote Sensing, 3(7:1552-1535.

Lu,D.& Weng,Q.,2009,Extraction of Urban Impervious Surfaces from an IKONOS Image, International Journal of , Remote Sensing, 30(5) , pp. 1297-1311.

Mohapatra, R.P.&Wu, C.,2008, Subpixel Imperviousness Estimation with IKONOS Imagery: An Artificial Neural Network Approach (pp.21-37).

Mohapatra, R.P. & Wu, C., 2010 High Resolution Impervious Surface Estimation. Photogrammetric Engineering & Remote Sensing, 76(12), pp, 1329-1341.

Powell, S.L., Cohen, W.B., Yang, Z., Pierce, I D. & Alberti, M., 2008, Quantification of Impervious Surface in the Snohomish Water Resources Inventory Area of Western Washington from 1972-2006, Remote Sensing Environment, 112(4), pp. 1895-1908.

Pu, R., Gong, P., Michishita, R.& Sasagawa, T.,2008, Spectral Mixture Analysis for Mapping Abundance of Urban Surface Components from the Terra /ASTER Data, Remote Sensing of Environment, 112(3), PP. 939-954.

Qin, Z., Karnieli, A. and Berliner, p., 2001. A mono-window algorithm for retrieving land surface temperature from Landsat TM data. International Journal of Remote Sensing.22(18): 3719-3746.

Qin, Z., Li, W. & Zhang, M. 2003. Estimating of the essential atmospheric parameters of mono-window algorithm for land surface temperature retrieaval from Landsat TM6. Remote Sensing for Land and Resources, 56: 37-43.

Rezaei, Akram, 2017, Extraction of the main factors affecting life in the city using spatial analysis (Case Study: Genaveh), Yazd Azad University, pp. 31-34.

SalmanMahini, AS. And Kamyab, h. 2009 Remote sensing and GIS applications with Idrisi software. Mehr Publication

Small, C.,2005, A Global Analysis of Urban Reflectance, International Journal of, Remote Sensing, 26(4), pp. 661-681.

Snyder, W. C. 1998. Classification based emissivity for land surface temperature measurement from space. International Journal of Remote Sensing, 19: 2753–2774.

Sobrino, J. A,.Jimenez-Munoz, J.C. & Paolini,L., 2004, Land Surface Temperature Retrieval Form LANDSAT TM 5 , , Remote Sensing of Environment , 90(4), pp. 434-440.

Song,Y.& Wu, C,.2016,Examining the Impact of Urban Biophysical Composition and Neighboring Environment on Surface Urban Heat Island Effect, Advances in Space Research ,57(1), pp.96-109.

Vogt,J. & Ohe,T.,2003,Termal Remot Sensing of Urban Climates, Remote sensing of Environment , 86(3) , pp.370-384.

Weng, Q., 2012, Remote Sensing of Impervious Surfaces in the Urban Areas:Requirements,Methods, and Trends, Remote Sensing of Environment ,117,pp.34-49.

Weng, Q.; Lu, D. & Schubring, J. 2004. Estimation of land surface temperature-vegetation abundance relationship for urban heat island studies. Remote Sensing of Environment, 89: 467-483.

Xiao J, Moody A. 2005. A comparison of methods for estimating fractional green vegetation cover within a desert-to-upland transition zone in central New Mexico, USA. Remote Sensing of Environment, 98(2-3): 237-250.

Yang, F.& Bauer, M.E.,2007, Comparison of Impervious Surface Area and Normalized Difference Vegetation Index as Indicators of Surface Urban Heat Island Effects in Landsat Imagery, Remote Sensing of Environment, 106(3), pp. 375-386.

Yang, H., & Liu, Y. (2005). A satellite remote sensing based assessment of urban heat island in Lanzhou city, northwest China. International Archives of Photogrammetry.Netherlands: Remote Sensing and Spatial Information Sciences.

Yang, X, 2006, Estimating Landscape Imagery, Geoscience and Remote Sensing Letters, IEEE, 3(1), PP.6-9.

Yang, X. & Liu, Z, 2005, Use of Satellite derved Landscape Imperviousness Index to Characterize Urban Spatial Growth, Computers, Environment and Urban Systems, 29(5), pp. 524-540.

Zhang, J.; Li, Y. & Wang, Y. 2007. Monitoring the urban heat island and the spatial expansion: using thermal remote sensing image of ETM+ band6, viewed 20 January 2011, www.sklog.labs. gov.cn/atticle/B07/B07023.pdf

Zhou Y, Weng Q, Gurney KR, Shuai Y, Hu X 2012. Estimation of the relationship between remotely sensed anthropogenic heat discharge and building energy use. ISPRS Journal of Photogrammetry and Remote Sensing, 67: 65-72.